Information Processing in Agriculture xxx (xxxx) xxx

Contents lists available at ScienceDirect

Information Processing in Agriculture

journal homepage: www.keaipublishing.com/en/journals/information-processing-in-agriculture/

Automated detection of larval stages of the black soldier fly (*Hermetia illucens* Linnaeus) through deep learning augmented with optical flow

Gianluca Manduca [a,b,*], Lloyd T. Wilson [c], Cesare Stefanini [a,b], Donato Romano [a,b,*]

[a] The BioRobotics Institute, Sant'Anna School of Advanced Studies, Viale R. Piaggio 34, 56025, Pontedera, Pisa, Italy
[b] Department of Excellence in Robotics and AI, Sant'Anna School of Advanced Studies, Piazza Martiri della Libertà 33, 56127 Pisa, Italy
[c] Texas A&M University and Texas A&M AgriLife Research, 1509 Aggie Drive, Beaumont, TX, USA

ARTICLE INFO

Keywords:
Precision techniques
Automated systems
Computer vision
Machine learning
Sustainability
Insect-based technologies

ABSTRACT

The black soldier fly (BSF) *Hermetia illucens* has garnered significant attention for its potential in sustainable waste management, nutrient recycling, and the production of valuable resources such as protein-rich animal feed and biofuels. Traditional mass production methods remain labor-intensive and error-prone, needing automated solutions. A critical challenge is the precise identification of BSF different life stages which is essential for optimizing feeding strategies, harvesting, and overall system efficiency. This study explores the use of deep learning, combined with optical flow analysis, to identify BSF life stages, particularly larvae, prepupae, and pupae. A Convolutional Neural Network (CNN) model was employed for real-time BSF larval stages detection. Training, validation, and test were performed on a comprehensive custom dataset of 2130 images. Evaluation metrics including precision, recall, and mean Average Precision (mAP) were assessed. Overall, the CNN model showed a precision of 0.96, a recall of 0.95, and a mAP@0.5 of 0.97 on the test set, confirming its generalization capability and effectiveness in real-world scenarios. The integration of optical flow enhanced the model's performance by leveraging prior knowledge of motor activity, particularly for identifying and correcting false positives in pupae classification. Automated identification of BSF larval stages optimizes resource management, reduces operational costs, and enhances the economic viability of BSF-based systems. The proposed system extends beyond terrestrial concerns, with potential implications for bioregenerative life-support systems, a promising space technology.

1. Introduction

In recent years, the black soldier fly (BSF) *Hermetia illucens* (Linnaeus) (Diptera: Stratiomyidae) has gained interest due to its potential in sustainable waste management [1,2], nutrient recycling [3], and the production of valuable resources like protein-rich animal feed and biofuels [4–6]. Traditionally, the mass production methods of *H. illucens* has mainly relied on manual methods, which are time-consuming, labor-intensive, and susceptible to human error [7,8], and few examples were based on automated approaches [9–11]. Recent studies have explored IoT-based solutions to optimize rearing conditions, demonstrating that automated environmental control can significantly enhance egg production by stabilizing temperature, humidity, and light intensity [12,13].

A critical aspect of effectively harnessing the potential of BSF lies in our ability to accurately distinguish between its different life stages, particularly the larvae, prepupae, and pupae [14,15]. This differentiation significantly influences various facets of BSF-based applications, including feeding strategies, harvesting methods, and overall operational success [16,17]. However, the classification of *H. illucens* life stages via automated learning approaches, is still unexplored. To overcome these challenges and to advance the precision and efficiency of BSF-related industries, a novel approach is required. In this context, the integration of artificial intelligence (AI) can offer an exciting and innovative solution.

AI-based technologies have been transformative in numerous scientific domains, offering the ability to automate complex tasks, analyze extensive datasets, and extract valuable insights [18–25]. AI models have shown great promise in various fields, including biological and ecological applications, with examples such as the early detection of Red

* Corresponding authors.
E-mail addresses: gianluca.manduca@santannapisa.it (G. Manduca), lt-wilson@aesrg.tamu.edu (L.T. Wilson), cesare.stefanini@santannapisa.it (C. Stefanini), donato.romano@santannapisa.it (D. Romano).

https://doi.org/10.1016/j.inpa.2025.05.001
Received 3 June 2024; Received in revised form 3 April 2025; Accepted 11 May 2025
Available online 14 May 2025

Palm Weevil larvae in palm trees [26] and the identification of Pacific oyster larvae [27]. The evolution of AI methods, including the integration of Transformers and Vision Transformers (ViTs), has further enhanced the ability to manage long-range dependencies, with applications spanning from Natural Language Processing (NLP) to computer vision and biological detection [28]. These continuing advances highlight the broad potential of AI to address complex challenges in various scientific applications.

In the case of *H. illucens*, AI and machine learning present the potential to redefine how we recognize, segregate, and manage the different life stages of the insect, with a particular focus on larvae, prepupae, and pupae. This approach can promote insect mass production technologies [29], enabling more sustainable circular economies [30]. Furthermore, the application of AI in the context of *H. illucens* and other edible insects extends beyond terrestrial concerns, with potential applications in space technology. The proposed approach plays a crucial role in enhancing bioregenerative life-support systems (BLSSs), which are essential for supporting prolonged space missions [31]. By leveraging AI to optimize insect life cycles and resource utilization, this methodology addresses Earthbound sustainability challenges and contributes to advancing our understanding of biologically regenerative systems essential for sustaining life beyond our planet [32].

This endeavor is significant for several key factors. Accurate identification of these larval stages optimizes resource management, which, in turn, enhances resource utilization, reduces operational costs, and promotes economic viability for BSF-based systems [33]. Efficient recognition of prepupae and pupae stages ensures timely collection of mature larvae, preventing premature pupation and maximizing their bioconversion potential, a key aspect of sustainable waste management [34–36]. For industries specializing in the utilization of BSF larvae for protein production or biofuel generation, precise separation of larval stages guarantees the delivery of high-quality and standardized end products [36,37].

The development of a reliable AI-based approach for identifying different larval stages in *H. illucens* not only has practical applications but also contributes to scientific advancements. It fosters a deeper understanding of the insect's biology, behavior, and development, which is instrumental for improving and diversifying its applications in various fields [38–40].

This study focuses on the innovative applications of deep learning in the identification of distinct larval stages in *H. illucens*, with a special emphasis on larvae, prepupae, and pupae. The employment of a Convolutional Neural Network (CNN) model trained on a comprehensive custom dataset is explored, discussing its potential to revolutionize the black soldier fly industry. A hybrid approach that integrates deep learning with optical flow is investigated. Integrating optical flow for motion analysis enhances CNN identification performance, as different larval stages exhibit varying motor activities. The workflow of the proposed approach is shown in Fig. 1. This technology aims to make the exploitation of *H. illucens* more efficient, sustainable, and economically viable, thus contributing to a greener and more thriving socioeconomic future.

2. Materials and methods

2.1. Animal rearing

Adult flies were bred under controlled laboratory conditions (27 ± 1.0 °C, 60 ± 10 % RH, 12:12 L:D) within nylon mesh fabric cages (90 x 50 x 50 cm). They were provided with *ad libitum* access to water and sugar cubes. Oviposition took place on corrugated cardboard surfaces, which were subsequently harvested and directly placed onto the substrate designated for larvae rearing. Larvae were accommodated in plexiglass boxes of dimensions 25 x 15 x 10 cm and nourished with the standard Gainesville diet [41]. Pupae underwent transfer to ventilated containers, and newly emerged adults were relocated to adult cages on a triweekly basis.

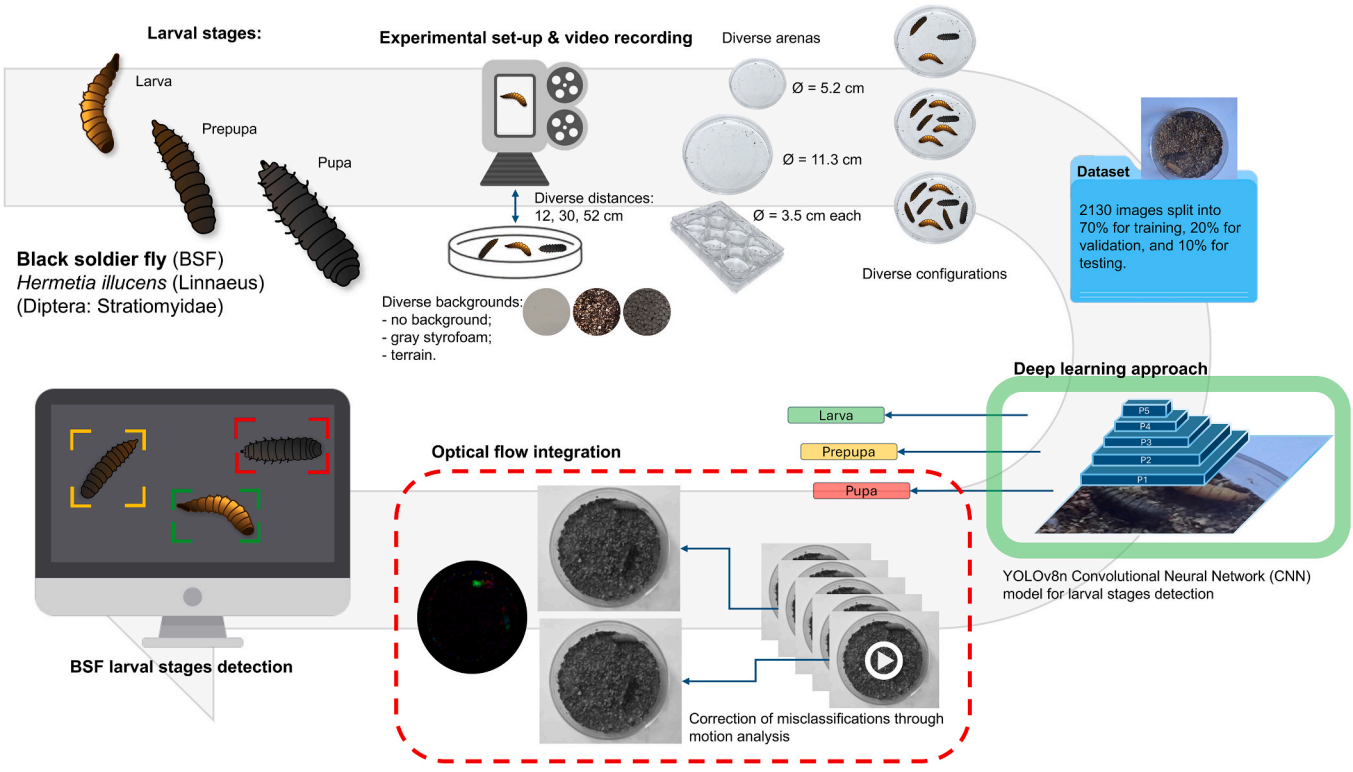

Fig. 1. Workflow of the proposed approach.

2.2. Experimental set-up and procedure

For image collection, a tripod was utilized, to which a 12 MP camera with a telephoto lens $f/2.8$ was attached. Various arenas were employed, including two circular arenas with diameters of 5.2 cm and 11.3 cm, and a structure composed of 6 circular arenas (Ø = 3,5 cm each). Different distances from the arena were evaluated: 12, 30, and 52 cm. Different backgrounds were evaluated: no background (white paper), gray styrofoam, and terrain.

Individual specimens were tested in the arena with a diameter of 5.2 cm, with different backgrounds and varying the distance between the camera and the arena. Subsequently, all possible pairings were examined, including larva-larva, pupa-pupa, prepupa-prepupa, larva-prepupa, larva-pupa, and prepupa-pupa. Finally, all three stages were concurrently investigated. In the arena with a diameter of 11.3 cm, various backgrounds and distances between the camera and the arena were considered to simultaneously examine a larger number of specimens, specifically 12 and 19, from different stages. Within the structure composed of six circular arenas, individual specimens from various stages were examined (one for each arena), with variations in the background and the distance between the camera and the arena. Subsequently, specimens from different stages were paired, exploring all possible combinations. Finally, pairings were randomized.

Various studies describe visually distinguishable traits between different larval stages [14]. Some distinct morphological and behavioral traits to differentiate between larval stages include a downward-curving labrum enabling prepupae to reach proper pupation sites, and their change in color from cream to black compared to younger larval stages. Beside color change, at pupal stage BSF also stops moving.

Individuals were recorded without external intervention. In instances where only pupae were present in the arena, the specimens were manually repositioned to capture different poses. A total of 65 videos, with a duration of around 5 min each, were recorded from 86 individuals (33 larvae, 27 prepupae, 26 pupae) at 30 fps with a resolution of 1920 x 1080 pixels. All recordings occurred between 09:00 and 24:00, at 22 ± 1 °C with laboratory light conditions, capturing individuals at various times of the day. This accounts for potential variations in lighting due to external conditions throughout the day. Frames were randomly extracted from video recordings, encompassing JPG and PNG file formats.

2.3. Dataset

This study collected 2130 images split into 70 % for training, 20 % for validation, and 10 % for testing, totaling 1491, 426, and 213 images, respectively. Images were manually labeled using the software available online makesense.ai. The dataset encompasses three distinct object categories (larva, prepupa, pupa), amounting to a total of 7350 object instances. The number of instances in each image varies from 1 to 19, representing different combinations of classes within the same image. The instances of the classes have been balanced to mitigate any potential bias towards any specific class. The instance distribution for each class is as follows: 2670 instances of larvae, 2430 instances of prepupae, and 2250 instances of pupae. The dataset includes a variety of backgrounds, different lighting conditions, various distances between the camera and the arena, a variety of combinations of individuals belonging to different classes within the arena, and different arena types. All these factors may influence the images and have been included to aid the model in generalization. Within the dataset, 180 background images have been included, also partitioned into 70 % for training, 20 % for validation, and 10 % for testing, totaling 126, 36, and 18 images, respectively. Data augmentation, a technique used to diversify training datasets and improve model generalization by artificially increasing the variety of training examples, was employed using the Python library Albumentations. This method applies a range of transformations, helping the model become more robust and capable of handling different real-world variations in the data. The augmentation process ensured a range of transformations, which helped mitigate overfitting and improved the model's ability to generalize on unseen data. The Mosaic method was applied, combining four resized images into a single mosaic to increase the diversity and complexity of training data. Both uniform box blur and median blur were applied, with the kernel size randomly chosen between 3 and 7 and a 0.01 probability of application. Median blur transform is particularly effective for noise reduction in image processing. Furthermore, grayscale conversion was applied with a 0.01 probability, as along with Contrast Limited Adaptive Histogram Equalization (CLAHE), with a clip limit of 4 and a tile grid size of 8 x 8, for additional augmentation.

2.4. Deep learning: CNN architecture and training

The Ultralytics YOLOv8n model has been selected for this study, leveraging the YOLO (You Only Look Once) family of CNNs for object detection [42]. YOLO has consistently demonstrated fidelity in real-time object detection and is characterized by its ability to perform the task in a single pass through the network, ensuring computational efficiency. These networks have been applied across a spectrum of detection tasks, and with a focus on the v8 version, ranging from marine species detection [43], to diagnosing various cancer types [44].

YOLOv8, an evolution in the YOLO family, integrates deep learning advancements for speed, detection performance, and ease of deployment. YOLOv8 Nano prioritizes compactness and real-time performance. YOLOv8 utilizes a modified CSPDarknet53 as its backbone, responsible for extracting features from input images. The network architecture employs C2f modules. The neck merges feature maps from various backbone stages. Finally, the head generates predictions using an anchor-free split Ultralytics head, improving both performance and efficiency compared to anchor-based methods. The network architecture is presented in Fig. 2. A pre-trained model on COCO dataset has been considered and fine-tuned on the developed custom dataset. The pre-trained network has a size of 6.24 MB, consisting of 225 layers, 3,011,433 parameters, 3,011,417 gradients, and a computational complexity of 8.2 GFLOPs. The following parameters were configured: batch size = 8, epochs = 200, patience = 15, and image size = 640 pixels. A Tesla T4 GPU was employed.

2.5. Performance metrics

In evaluating the CNN model performance different metrics were considered.

Precision refers to the probability of correctly predicting positive samples among the predicted positive samples. Precision is computed as follows:

$$Precision = \frac{TP}{TP + FP} \tag{1}$$

The variable TP denotes the count of true positives, while FP represents the count of false positives. This metric is important since it is an indicator of the quality of a positive prediction made by the model. High precision ensures that when the model predicts a particular larval stage, the prediction is highly reliable, minimizing the occurrence of false positives. This is especially important in the context of our application, as misclassification of a larval stage could result in inefficiencies in resource allocation and management. Optimization for precision ensures that the model is both sensitive to detecting different stages and highly accurate in its identification, which is critical for practical deployment in automated systems.

Recall represents the probability of correctly predicting positive samples among all actual positive samples. It is calculated as follows:

$$Recall = \frac{TP}{TP + FN} \tag{2}$$

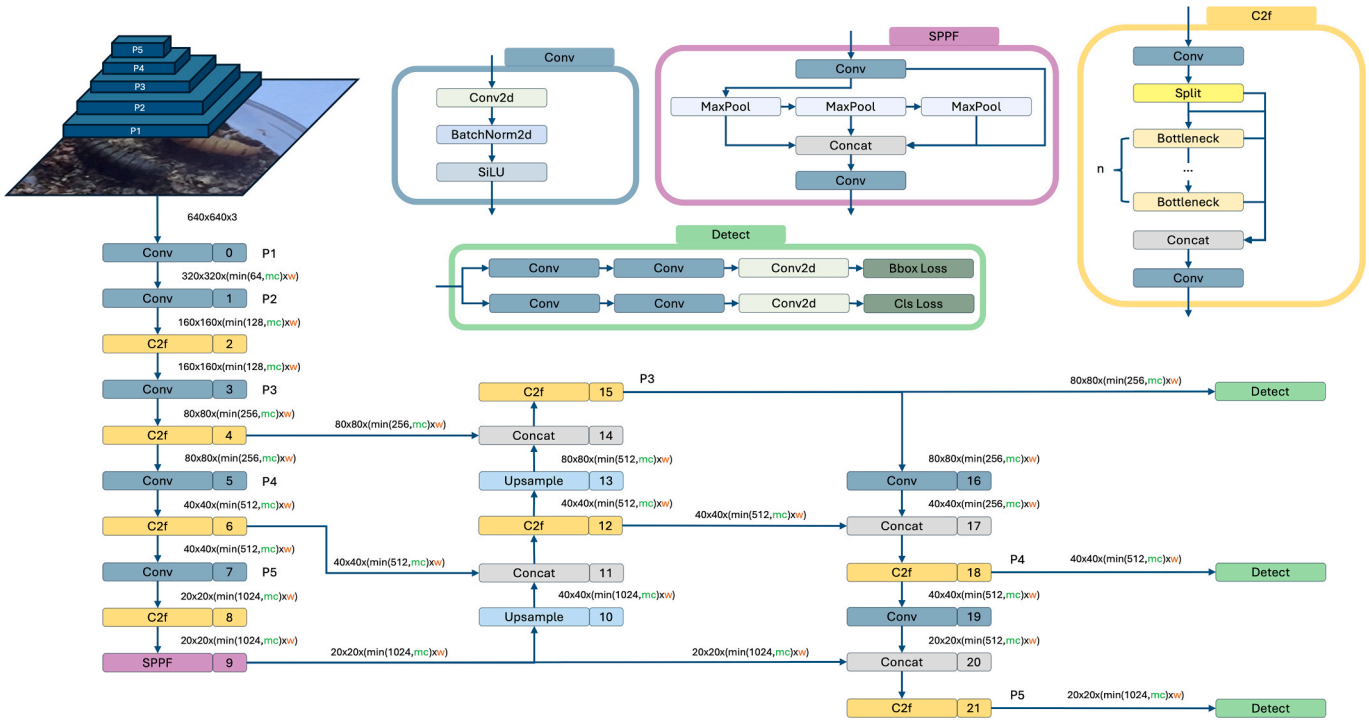

Fig. 2. YOLOv8 detection model architecture: The width multiple (w) and max channels (mc) parameters determine the number of channels at each layer. The CNN model considered (YOLOv8n) has w = 0.25 and mc = 1024.

The variable FN represents the count of false negatives.

The F1-score provides the harmonic mean of precision and recall, thus offering a balanced evaluation between them. It is computed as follows:

$$F1 - Score = 2 \bullet \frac{Precision \bullet Recall}{Precision + Recall} \tag{3}$$

The Average Precision (AP) calculates the area under the precision-recall curve, providing a single value that represents the model's performance in terms of both precision and recall. The mean Average Precision (mAP) expands the concept of AP by computing the average AP values across multiple object classes. mAP is calculated using the following formula:

$$mAP = \frac{\sum_{i=1}^{N} AP_i}{N} \tag{4}$$

N represents the total number of classes, and AP_i denotes the Average Precision of class i. mAP@0.5 is the mean Average Precision at an Intersection over Union (IoU) threshold of 0.5. mAP@0.5:0.95 represents the mean Average Precision calculated at different IoU thresholds, ranging from 0.50 to 0.95.

During training, Box Loss measures bounding box accuracy by assessing deviation from ground truth. Class Loss evaluates classification performance by measuring the difference between predicted class probabilities and actual labels. Distribution Focal Loss (DFL) is used for fine-grained classification.

2.6. Optical flow

This study integrates a CNN detection model with motion analysis to enhance performance, leveraging prior knowledge of class-specific motor activity. Pupae, for instance, typically exhibit minimal motor activity compared to other classes. Optical flow analysis using the Farnebäck algorithm was employed for motion analysis [45]. Optical flow estimates the motion among two frames. The frame intensity $I(x, y, t)$ can be expressed as a function of space and time. In the second frame, the intensity moves by a distance (dx, dy) after a time step dt. Assuming constant object pixel intensities between consecutive frames, it results:

$$I(x, y, t) = I(x + dx, y + dy, t + dt) \tag{5}$$

Applying a first-order Taylor series expansion, it results:

$$f_x u + f_y v + f_t = 0 \tag{6}$$

where

$$f_x = \frac{\partial I}{\partial x}, f_y = \frac{\partial I}{\partial y}, f_t = \frac{\partial I}{\partial t} \tag{7}$$

and

$$u = \frac{dx}{dt}, v = \frac{dy}{dt} \tag{8}$$

f_x, f_y, and f_t are the image gradients along the x-axis, y-axis, and time, respectively. u and v are the unknowns representing the optical flow in the x and y directions.

The Farnebäck method solves **Eq. (6)** by applying polynomial expansion so that some neighborhoods of each pixel are approximated by using a quadratic polynomial:

$$F_1(X) = X^T A_1 X + {b_1}^T X + c_1 \tag{9}$$

where $X = (x, y)^T$.

A new signal $F_2(X)$ is constructed over a displacement d:

$$\begin{aligned} F_2(X) = F_1(X - d) &= (X - d)^T A_1 (X - d) + {b_1}^T (X - d) + c_1 \\ &= X^T A_1 X + (b_1 - 2A_1 d)^T X + d^T A_1 d - {b_1}^T d + c_1 \\ &= X^T A_2 X + {b_2}^T X + c_2 \end{aligned} \tag{10}$$

where

$$A_2 = A_1 \tag{11}$$

$$b_2 = b_1 - 2A_1 d \tag{12}$$

$$c_2 = d^T A_1 d - {b_1}^T d + c_1 \tag{13}$$

From **Eq. (12)**, in cases where A_1 is non-singular, the translation d can be computed:

$$d = -\frac{1}{2}{A_1}^{-1}(b_2 - b_1) \tag{14}$$

Images were converted from RGB to grayscale before computing optical flow, focusing solely on motion magnitude. The Python OpenCV library's calcOpticalFlowFarneback() function was utilized with specific parameter configurations: scale = 0.5, pyramid layers = 5, averaging window size = 15, iterations = 3, polynomial expansion pixel neighborhood size = 7, and Gaussian standard deviation for derivative smoothing = 1.5. This method was integrated with deep learning detection, considering only magnitude values within identified bounding boxes. A threshold was established to differentiate motor activity between pupae and prepupae/larvae. Four 3-minute videos were analyzed, featuring different set-ups, including various backgrounds (white surface and gray styrofoam) and distances between the camera and the arenas (30 cm and 52 cm). The videos considered for the analysis featured either the structure with six circular arenas (Ø = 3.5 cm each) or the single larger circular arena (Ø = 11.3 cm), with 12 individuals present in each video.

Optical flow was computed for each video by comparing consecutive frames at different sampling frequencies: 1 Hz, 0.5 Hz, and 0.25 Hz. For each frame in the videos, the mean magnitude within bounding boxes was computed post-detection. Subsequently, bounding boxes with the lowest and highest mean optical flow magnitude values were considered to discern pupae motor activity from other classes. A single threshold was defined for all scenarios. False positives in pupae classification were addressed by comparing the mean magnitudes within bounding boxes to this threshold. CNN model predictions were adjusted when the mean magnitudes exceeded the defined threshold. To ensure accurate detection augmentation, optical flow analysis was omitted when pupae movements appeared influenced by crowded environments. Specifically, situations were excluded where the center of the bounding box of an identified individual overlapped with the bounding box of the individual under examination.

3. Results

The CNN model's detection performance was assessed, with Fig. 3 showing performance metrics during training and validation. A typical trend in training involves a systematic decrease in loss metrics, indicating the model's adaptive learning dynamics. This reduction reflects the model's ability to iteratively adjust parameters and improve proficiency in identifying complex patterns within the dataset. The precision, recall, and mAP of the model exhibited improvement over the epochs before stabilizing at epoch 180. Training was stopped early due to a lack of improvement in validation loss over the last 15 epochs, indicating that the model had reached its optimal performance and further training would risk overfitting. This approach allowed us to effectively manage training duration while minimizing the risk of overfitting and ensuring the model's ability to generalize. 180 epochs were completed in 1.819 h with a Tesla T4 GPU. Best results were observed at epoch 165. The optimal network configuration has 225 layers, a total of 3,011,433 parameters, and a computational complexity of 8.2 GFLOPs. Overall, the proposed approach achieved a precision of 0.98, a recall of 0.93, and a

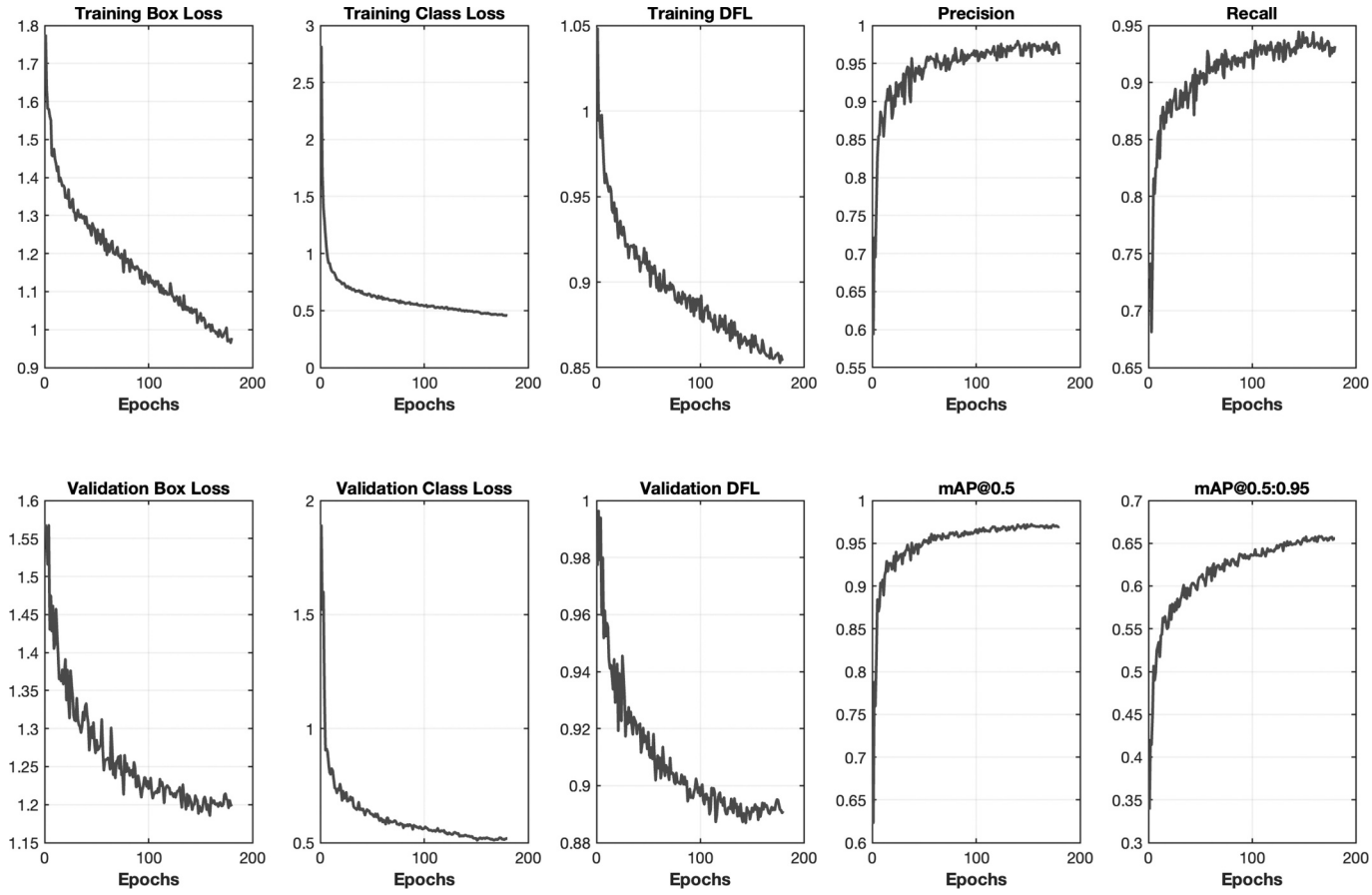

Fig. 3. Training and validation results: Visualization across epochs of different metrics including Box Loss, Class Loss and DFL, precision, recall, mAP@0.5 and mAP@0.5:0.95.

mAP@0.5 of 0.97 on the validation set. The network showed a precision of 1.00 at 0.87 confidence, and a recall of 0.97 at 0.00 confidence. The F1-score reached 0.95 at 0.48. The best model configuration was applied on the test set, consisting of 213 images corresponding to 735 instances of larvae (266), prepupae (245), and pupae (224). Overall, the network achieved a precision of 0.96, a recall of 0.95, and a mAP@0.5 of 0.97 on the test set. The network showed a precision of 1.00 at 0.91 confidence, and a recall of 0.97 at 0.00 confidence. The F1-score reached 0.96 at 0.44. The results align with those obtained on the validation set, demonstrating that the network has generalized and not overfitted during the training phase.

Fig. 4 shows the precision-recall curves (**A**) together with normalized confusion matrix (**B**) obtained. Observing the precision-recall curves, the mAP@0.5 values of 0.97 (larva), 0.96 (prepupa), and 0.99 (pupa) highlight the model's high precision and recall capabilities. These metrics indicate the model's proficiency in accurately distinguishing between positive and negative instances, reflecting its sensitivity in correctly identifying objects of interest. Precision-recall curves with values approaching 1.00 further emphasize that the model has struck an optimal balance between precision and recall. This evaluation is crucial in object detection applications, particularly in scenarios where minimizing both false positives and false negatives is imperative for reliable and accurate results.

Analyzing the normalized confusion matrix, the CNN achieved a precision of 0.95 and a recall of 0.97 for the larva class, with 0.03 of larvae misclassified as background. For the prepupa class, the CNN attained a precision of 0.94 and a recall of 0.95, with 0.02 of prepupae misclassified as pupae and 0.03 as background. Regarding the pupa class, the CNN achieved a precision of 0.93 and a recall of 0.98, with 0.01 of pupae misclassified as prepupae and another 0.01 as background. Overall, the CNN demonstrated consistent performance on the larva and pupa classes, with minimal misclassification into the background category. Although the CNN maintained high precision and recall on the prepupa class, it showed slightly higher misclassification rates compared to the larva and pupa classes. The matrix suggests that the model performed effectively in classifying the different classes, with only small errors.

The CNN exhibits strong performance overall, achieving an inference time of 6.10 ms on the test set. The normalized confusion matrix reveals slightly greater difficulty in distinguishing between pupae and prepupae, with prepupae occasionally misclassified as pupae with an error rate of 0.02. To improve performance, the proposed approach leverages motion analysis via optical flow, enhancing automatic detection at the video level. By comparing consecutive frames, false positives in pupae classification can be identified and corrected by assigning them to the prepupa class. Fig. 5 illustrates the definition of the optical flow magnitude threshold, crucial for distinguishing pupae's minimal motor activity from that of prepupae/larvae. Two consecutive frames were transformed from RGB to grayscale, and the Farnebäck algorithm for optical flow was applied. By integrating this approach with detection, the focus shifts to individuals' motor activity, defining their motion magnitude. Fig. 5(**A**) illustrates the adopted approach, comparing frames sampled at 1 Hz, performing detection on the second frame, and presenting magnitude through MINMAX normalization. Panels (**B**), (**C**), and (**D**) demonstrate optical flow magnitude differences among pupae and other classes at varying sampling frequencies (1 Hz, 0.5 Hz, and 0.25 Hz). As the sampling frequency decreases, the optical flow magnitude increases, with a particularly noticeable effect in prepupae and larvae. In contrast, the magnitude for pupae remains consistently below the threshold of 1 pixel across all frequencies. Testing on four videos at 1 Hz confirms the effectiveness of the approach. Fig. 5(**F**) depicts detection results without (top row) and with (bottom row) corrections, showing improvements in most scenarios. The CNN model, integrated with optical flow analysis, exhibits enhanced performance.

4. Discussion

The use of a CNN model augmented with optical flow represents a pioneering advancement in automated detection of black soldier fly (BSF) *H. illucens* larval stages, contributing to insect-based sustainable technologies. YOLOv8's real-time object detection proficiency across various domains, coupled with its computational efficiency, justifies its selection [42,43]. Optical flow integration further enhances the model's ability by accurately capturing dynamic movements inherent in BSF larval stages, which is particularly useful for distinguishing behavioral patterns between larvae, prepupae, and pupae, thereby improving identification performance. Our iterative training approach, spanning 180 epochs, aimed to balance model underfitting and overfitting. Early stopping was considered to prevent overfitting and ensure model generalization across different larval stage variations. Overall, the CNN achieved a precision of 0.98, a recall of 0.93, and a mAP@0.5 of 0.97 on the validation set highlighting the model's strong performance in identifying BSF larval stages. Results on the test set affirm the model's generalization capacity, ensuring robust performance in real-world applications. The normalized confusion matrix indicates the model's ability to distinguish between larva, prepupa, and pupa classes with

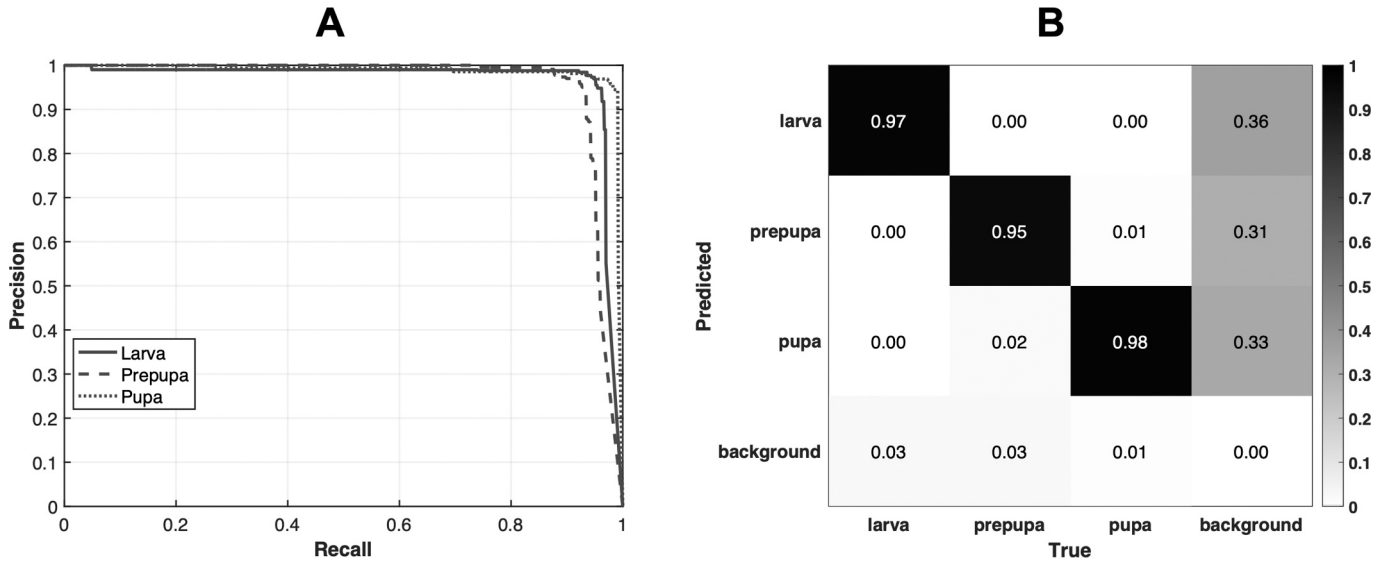

Fig. 4. Test results: Precision-recall curves (**A**), and normalized confusion matrix (**B**).

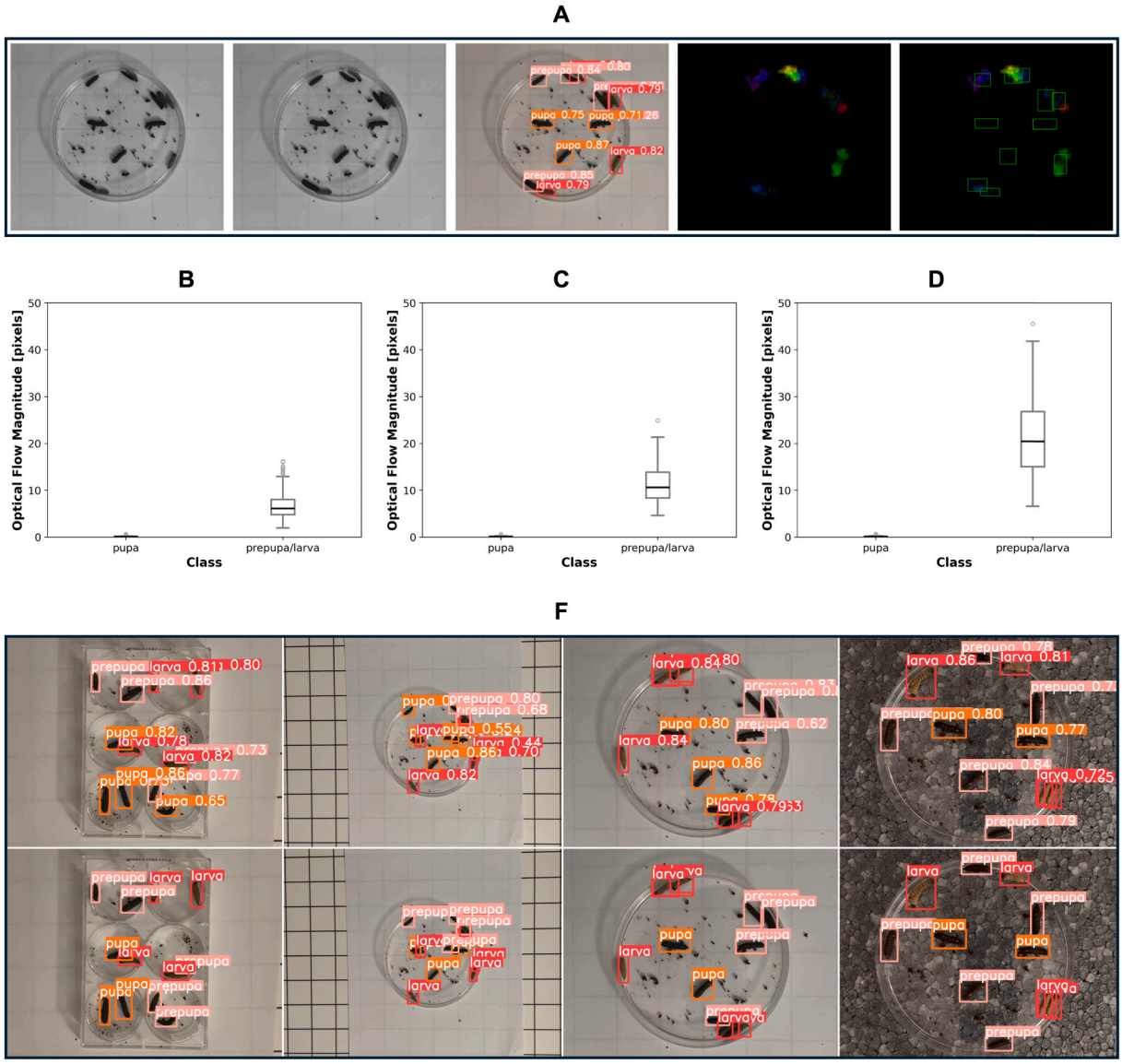

Fig. 5. Optical flow magnitude threshold determination and integration results: Comparison of two consecutive frames sampled at 1 Hz, detection performed on the second frame to determine bounding boxes, graphical representation of optical flow magnitudes normalized using MINMAX scaling, and bounding boxes overlaid on the graphical representation (**A**); comparison of optical flow magnitude between pupae and other classes at sampling frequencies of 1 Hz (**B**), 0.5 Hz (**C**), and 0.25 Hz (**D**); detection results before (top row) and after (bottom row) corrections using optical flow, shown for a single frame from each of the four analyzed videos (one per column) (**F**).

minimal errors. While the CNN achieved excellent performance on the larva and pupa classes, it exhibited slightly higher errors in the classification of the prepupa class, indicating areas for improvement. These findings corroborate the effectiveness and versatility of deep learning methodologies across different domains and applications. Precision-recall curves with mAP@0.5 values of 0.97 (larva), 0.96 (prepupa), and 0.99 (pupa) underscore the model's precision and recall capabilities. These metrics highlight the model's sensitivity in correctly identifying positive instances while minimizing false positives and false negatives. Additionally, the model's inference time of 6.10 ms on the test set enables real-time detection for field applications.

The results achieved in this study are consistent with previous research employing deep learning for detection tasks [46]. For instance, in [47] proposed a hybrid deep learning algorithm, combining CNNs and Gated Recurrent Units (GRU), to enhance security in the Smart Grid by detecting Distributed Denial of Service (DDoS) attacks, surpassing traditional intrusion detection methods. In [48], an automated blue whale D-call detector using DenseNet, trained on Antarctic acoustic recordings, was developed. A double-observer analysis showed that the automated detector outperformed human analysts, with higher recall and fewer false positives. A deep learning approach for detecting and counting Pacific oyster larvae was introduced in [27], which also enabled accurate estimation of larval shell height. In the context of pest management, a YOLOv8s model integrated within a smart trap successfully identified multiple species of hematophagous flies, demonstrating robust performance [49]. In [50], a deep neural network was developed for identifying *Aedes aegypti* and *Aedes albopictus* larvae, achieving results comparable to those in this study and incorporating automated region of interest (ROI) cropping and rapid classification, offering a cost-effective solution for mosquito control.

The introduction of Transformers, leveraging self-attention mechanisms to manage long dependencies in sequential data, has marked a transformative shift in AI research, expanding applications across fields such as NLP, computer vision, and biological detection [28]. For

instance, in plant recognition tasks, the application of ViTs has notably enhanced both performance and efficiency [51]. Additionally, ViT models have been applied to crop pest image recognition [52], further demonstrating their versatility. These studies highlight the potential of deep learning and advanced architectures in tackling challenges in biosystems engineering.

The integration of optical flow enhances the CNN performance by leveraging insights into the motor activity of BSF larval stages. Optical flow analysis provides deeper understanding of motion patterns, enabling precise identification and correction of false positives, especially in pupae classification, by reassigning them to the prepupa class. This integration allows the model to adapt predictions based on small movement changes, leading to improved performance and robustness in BSF larval stage detection.

The key contribution of this work is the automation of the larval stage identification process. The CNN model is capable of distinguishing larval stages that are difficult to differentiate with the human eye, particularly in the case of pupae/prepupae. Additionally, the proposed methodology is innovative as it integrates an enhanced deep learning approach with optical flow analysis. A similar hybrid approach has been proposed combining microfluidics, deep learning, and optical flow to analyze the behavior of *Steinernema carpocapsae* entomopathogenic nematodes (EPNs) in response to stimuli [53]. The integration of optical flow analysis further revealed significant variations in motor activity, providing valuable insights into the dynamic responses of EPNs and enhancing the understanding of their behavior for improved biocontrol strategies.

The trained CNN model, enhanced with optical flow, autonomously recognizes larval stages, significantly reducing the time and resources required from human operators who would otherwise perform this task manually. Automation, as seen in many industrial processes, plays an important role in improving efficiency, minimizing errors, and cutting operational costs. In the context of *H. illucens* breeding, this model facilitates a more streamlined and consistent workflow, allowing large-scale production systems to operate with higher precision and sustainability.

Accurate identification of BSF larval stages holds significant promise for optimizing resource utilization and reducing operational costs in biosystems focused on sustainable waste management [54–56]. Industries specializing in utilizing BSF larvae for protein production or biofuel generation can benefit from the precise separation of larval stages, ensuring high-quality and standardized end products. Furthermore, the application of AI in the context of BSF and edible insects has implications beyond terrestrial concerns, particularly in BLSSs [57]. The model's potential role in enhancing these systems is crucial for prolonged space missions, aligning with the interdisciplinary nature of biosystems engineering [31,58–60].

Ongoing efforts in refining the model architecture, training strategies, and incorporating feedback from real-world applications are essential for continuous improvement. This iterative optimization process aligns with the interdisciplinary nature of biosystems engineering, ensuring the relevance and efficacy of the automated detection system.

5. Conclusions

This study demonstrated the effectiveness of a deep learning model combined with optical flow in automatically detecting BSF larval stages, offering a reliable alternative to traditional manual methods prone to errors. The CNN showed excellent performance, with high precision, recall, and mAP scores, proving its ability to reliably identify BSF larvae, prepupae, and pupae in real-world conditions. The network differentiated larval stages that were challenging to distinguish through traditional visual inspection. The optical flow integration helped improve the model's performance, especially when distinguishing between prepupae and pupae, where movement patterns play a crucial role. The proposed approach turns out to be both innovative and effective. This automated system improves efficiency by reducing errors and saving time in BSF applications. Its implementation can optimize resource management, simplify operational processes, and ensure high-quality mass production for industries utilizing BSF in protein, biofuel, and waste processing applications. Moreover, the ability to accurately classify BSF life stages can refine harvesting and feeding strategies, maximizing bioconversion potential while minimizing costs. Additionally, the model could have applications beyond Earth, particularly in space, where it could contribute to bioregenerative life support systems. Future work should focus on expanding the dataset and testing the model in real-world environments to validate its robustness across different conditions and scenarios.

CRediT authorship contribution statement

Gianluca Manduca: Writing – review & editing, Writing – original draft, Visualization, Validation, Software, Methodology, Investigation, Formal analysis, Data curation, Conceptualization. **Lloyd T. Wilson:** Writing – review & editing, Formal analysis. **Cesare Stefanini:** Writing – review & editing, Investigation, Formal analysis. **Donato Romano:** Writing – review & editing, Writing – original draft, Visualization, Validation, Supervision, Resources, Project administration, Methodology, Investigation, Funding acquisition, Formal analysis, Data curation, Conceptualization.

Funding

The PRIN Project "COSMIC - COntrolled Space MIcroecological system supporting eCopoiesis" granted by the Italian Ministry of Education, University and Research (MIUR) [2022EY5BXC].

Declaration of competing interest

The authors declare that they have no known competing financial interests or personal relationships that could have appeared to influence the work reported in this paper.

Acknowledgments

This research was supported by the PRIN 2022 Project "COSMIC—COntrolled Space MIcroecological system supporting eCopoiesis" [Project Code:2022EY5BXC], the Italian Space Agency (ASI) DC-DSR-UVS-2022-375 Project "pRomoting pEdogenesis throuGh lunar sOil-terrestriaL organIsms interaction For moon Fertilization – REGOLIFE" [ASI N.: 2024-7-U.0; CUP: J83C24000310005], and BRIEF "Biorobotics Research and Innovation Engineering Facilities" (project identification code IR0000036), project funded under the National Recovery and Resilience Plan (NRRP), Mission 4 Component 2 Investment 3.1 of Italian Ministry of University and Research funded by the European Union – NextGenerationEU. Funders had no role in the study design, data collection and analysis, decision to publish, or preparation of the manuscript. The authors thank Cristina Piras for her kind assistance in visualization.

Data availability

Data will be shared upon request.

References

[1] Bulak P, Polakowski C, Nowak K, Waśko A, Wiącek D, Bieganowski A. *Hermetia illucens* as a new and promising species for use in entomoremediation. Sci Total Environ 2018;633:912–9. https://doi.org/10.1016/j.scitotenv.2018.03.252.

[2] da Silva GDP, Hesselberg T. A review of the use of black soldier fly larvae, *Hermetia illucens* (Diptera: Stratiomyidae), to compost organic waste in tropical regions. Neotrop Entomol 2020;49(2):151–62. https://doi.org/10.1007/s13744-019-00719-z.

[3] Smetana S, Schmitt E, Mathys A. Sustainable use of *Hermetia illucens* insect biomass for feed and food: Attributional and consequential life cycle assessment. Resour Conserv Recycl 2019;144:285–96. https://doi.org/10.1016/j.resconrec.2019.01.042.
[4] Nairuti RN, Musyoka SN, Yegon MJ, Opiyo MA. Utilization of black soldier fly (*Hermetia illucens* Linnaeus) larvae as a protein source for fish feed–a review. Aquaculture Studies 2021;22(2). https://doi.org/10.4194/AQUAST697.
[5] Mangindaan D, Kaburuan ER, Meindrawan B. Black soldier fly larvae (*Hermetia Illucens*) for biodiesel and/or animal feed as a solution for waste-food-energy nexus: Bibliometric analysis. Sustainability 2022;14(21):13993. https://doi.org/10.3390/su142113993.
[6] Mohan K, Sathishkumar P, Rajan DK, Rajarajeswaran J, Ganesan AR. Black soldier fly (*Hermetia illucens*) larvae as potential feedstock for the biodiesel production: Recent advances and challenges. Sci Total Environ 2023;859:160235. https://doi.org/10.1016/j.scitotenv.2022.160235.
[7] Ortiz JC, Ruiz AT, Morales-Ramos JA, Thomas M, Rojas MG, Tomberlin JK, et al. In: Insect mass production technologies. Academic Press; 2016. p. 153–201. https://doi.org/10.1016/B978-0-12-802856-8.00006-5.
[8] Pintowantoro S, Setiyorini Y, Aljauhari AM, Abdul F, Nurdiansah H. Black soldier fly biowaste treatment and its recycle waste to produce chitosan. In IOP Conference Series. In: Earth and Environmental Science. 649. IOP Publishing; 2021, 012004. https://doi.org/10.1088/1755-1315/649/1/012004.
[9] Erbland P, Alyokhin A, Peterson M. An automated incubator for rearing black soldier fly larvae (*Hermetia illucens*). Trans ASABE 2021;64(6):1989–97. https://doi.org/10.13031/trans.14623.
[10] Pahmeyer MJ, Siddiqui SA, Pleissner D, Gołaszewski J, Heinz V, Smetana S. An automated, modular system for organic waste utilization using *Hermetia illucens* larvae: Design, sustainability, and economics. J Clean Prod 2022;379:134727. https://doi.org/10.1016/j.jclepro.2022.134727.
[11] Yu G, Nishi H, Pang C, Gu Q, Lin Y, Liang J, Dai W, Vyatkin V. Black Soldier Fly Bioconversion System: A Digital Twin Approach. In 2023 IEEE 32nd International Symposium on Industrial Electronics (ISIE); 2023. p. 1–4. https://doi.org/10.1109/ISIE51358.2023.10227952.
[12] Kristianto K, Lambert RV, Girsang AS. Automated IoT Device to Manipulate Environmental Condition of Black Soldier Fly. International Journal of Emerging Technology and Advanced Engineering 2022;12:33–40. https://doi.org/10.46338/ijetae0322_05.
[13] Girsang AS, Kaburuan ER, Peranginangin E, Kristianto K, Lambert RV, Yunanda R. Black soldier fly (BSF) farming in egg cycle based on IoT technology. In: AIP Conference Proceedings. 2867. AIP Publishing; 2024. p. 030022. https://doi.org/10.1063/5.0225243.
[14] Barros LM, Gutjahr ALN, Ferreira-Keppler RL, Martins RT. Morphological description of the immature stages of *Hermetia illucens* (Linnaeus, 1758) (Diptera: Stratiomyidae). Microsc Res Tech 2019;82(3):178–89. https://doi.org/10.1002/jemt.23127.
[15] Padmanabha M, Kobelski A, Hempel AJ, Streif S. A comprehensive dynamic growth and development model of *Hermetia illucens* larvae. PLoS One 2020;15(9):e0239084. https://doi.org/10.1371/journal.pone.0239084.
[16] Lanes CF, Pedron FA, Bergamin GT, Bitencourt AL, Dorneles BE, Villanova JC, et al. Black Soldier Fly (*Hermetia illucens*) larvae and prepupae defatted meals in diets for zebrafish (*Danio rerio*). Animals 2021;11(3):720. https://doi.org/10.3390/ani11030720.
[17] Kaczor M, Bulak P, Proc-Pietrycha K, Kirichenko-Babko M, Bieganowski A. The Variety of Applications of *Hermetia illucens* in Industrial and Agricultural Areas. Biology 2022;12(1):25. https://doi.org/10.3390/biology12010025.
[18] Smith MJ. Getting value from artificial intelligence in agriculture. Anim Prod Sci 2018;60(1):46–54. https://doi.org/10.1071/AN18522.
[19] Føre M, Frank K, Norton T, Svendsen E, Alfredsen JA, Dempster T, et al. Precision fish farming: A new framework to improve production in aquaculture. Biosyst Eng 2018;173:176–93. https://doi.org/10.1016/j.biosystemseng.2017.10.014.
[20] Jha K, Doshi A, Patel P, Shah M. A comprehensive review on automation in agriculture using artificial intelligence. Artif Intell Agric 2019;2:1–12. https://doi.org/10.1016/j.aiia.2019.05.004.
[21] Ellahham S, Ellahham N, Simsekler MCE. Application of artificial intelligence in the health care safety context: opportunities and challenges. Am J Med Qual 2020;35(4):341–8. https://doi.org/10.1177/1062860619878515.
[22] Peres RS, Jia X, Lee J, Sun K, Colombo AW, Barata J. Industrial artificial intelligence in industry 4.0-systematic review, challenges and outlook. IEEE Access 2020;8:220121–39. https://doi.org/10.1109/ACCESS.2020.3042874.
[23] Liu X, Du K, Zhang C, Luo Y, Sha Z, Wang C. Precision feeding system for largemouth bass (*Micropterus salmoides*) based on multi-factor comprehensive control. Biosyst Eng 2023;227:195–216. https://doi.org/10.1016/j.biosystemseng.2023.02.005.
[24] Manduca G, Zeni V, Moccia S, Milano BA, Canale A, Benelli G, Stefanini C, Romano D. Learning algorithms estimate pose and detect motor anomalies in flies exposed to minimal doses of a toxicant. iScience 2023;26(12). https://doi.org/10.1016/j.isci.2023.108349.
[25] Romano D. Novel Automation, AI, and Biomimetic Engineering Advancements for Insect Studies and Management. Curr Opin Insect Sci 2025;101337. https://doi.org/10.1016/j.cois.2025.101337.
[26] Mohamed A, Hany A, Adly I, Atwa A, Ragai H. AI for Acoustic Early Detection of the Red Palm Weevil. In: In 2021 16th International Conference on Computer Engineering and Systems (ICCES). IEEE; 2021. https://doi.org/10.1109/ICCES54031.2021.9686081.
[27] Kakehi S, Sekiuchi T, Ito H, Ueno S, Takeuchi Y, Suzuki K, et al. Identification and counting of Pacific oyster *Crassostrea gigas* larvae by object detection using deep learning. Aquac Eng 2021;95:102197. https://doi.org/10.1016/j.aquaeng.2021.102197.
[28] Islam S, Elmekki H, Elsebai A, Bentahar J, Drawel N, Rjoub G, et al. A comprehensive survey on applications of transformers for deep learning tasks. Expert Syst Appl 2024;241:122666. https://doi.org/10.1016/j.eswa.2023.122666.
[29] Melgar-Lalanne G, Hernández-Álvarez AJ, Salinas-Castro A. Edible insects processing: Traditional and innovative technologies. Compr Rev Food Sci Food Saf 2019;18(4):1166–91. https://doi.org/10.1111/1541-4337.12463.
[30] Barragán-Fonseca KB, Muñoz-Ramírez AP, Mc Cune N, Pineda J, Dicke M, Cortés J. Fighting rural poverty in Colombia: Circular agriculture by using insects as feed in aquaculture. Wageningen Livestock Research. Report / Wageningen Livestock Research No 1153; 2022. https://doi.org/10.18174/561878.
[31] Metelli G, Lampazzi E, Pagliarello R, Garegnani M, Nardi L, Calvitti M, et al. Design of a modular controlled unit for the study of bioprocesses: Towards solutions for Bioregenerative Life Support Systems in space. Life Sci Space Res 2023;36:8–17. https://doi.org/10.1016/j.lssr.2022.10.006.
[32] De Micco V, Amitrano C, Mastroleo F, Aronne G, Battistelli A, Carnero-Diaz E, et al. Plant and microbial science and technology as cornerstones to Bioregenerative Life Support Systems in space. npj Microgravity 2023;9(1):69. https://doi.org/10.1038/s41526-023-00317-9.
[33] Surendra KC, Tomberlin JK, van Huis A, Cammack JA, Heckmann LHL, Khanal SK. Rethinking organic wastes bioconversion: Evaluating the potential of the black soldier fly (*Hermetia illucens* (L.)) (Diptera: Stratiomyidae) (BSF). Waste Manag 2020;117:58–80. https://doi.org/10.1016/j.wasman.2020.07.050.
[34] Chia SY, Tanga CM, Khamis FM, Mohamed SA, Salifu D, Sevgan S, et al. Threshold temperatures and thermal requirements of black soldier fly *Hermetia illucens*: Implications for mass production. PLoS One 2018;13(11):e0206097. https://doi.org/10.1371/journal.pone.0206097.
[35] Ravi HK, Degrou A, Costil J, Trespeuch C, Chemat F, Vian MA. Larvae mediated valorization of industrial, agriculture and food wastes: Biorefinery concept through bioconversion, processes, procedures, and products. Processes 2020;8(7):857. https://doi.org/10.3390/pr8070857.
[36] Bosch G, Oonincx DGAB, Jordan HR, Zhang J, van Loon JJA, van Huis A, et al. Standardisation of quantitative resource conversion studies with black soldier fly larvae. J Insects Food Feed 2020;6(2):95–109. https://doi.org/10.3920/JIFF2019.0004.
[37] Caligiani A, Marseglia A, Leni G, Baldassarre S, Maistrello L, Dossena A, et al. Composition of black soldier fly prepupae and systematic approaches for extraction and fractionation of proteins, lipids and chitin. Food Res Int 2018;105:812–20. https://doi.org/10.1016/j.foodres.2017.12.012.
[38] Hoc B, Noël G, Carpentier J, Francis F, Caparros Megido R. Optimization of black soldier fly (*Hermetia illucens*) artificial reproduction. PLoS One 2019;14(4):e0216160. https://doi.org/10.1007/s11367-021-01986-y.
[39] Bogdan G, Ioan SD, Mihai Ş, Elena ML, Vasile MD, Mihaela BA. Particularities of the *Hermetia illucens* (L.) (Diptera: Stratiomyidae) Ovipositing Behavior: Practical Applications. Insects 2022;13(7):611. https://doi.org/10.3390/insects13070611.
[40] Meneguz M, Miranda CD, Cammack JA, Tomberlin JK. Adult behaviour as the next frontier for optimising industrial production of the black soldier fly *Hermetia illucens* (L.) (Diptera: Stratiomyidae). J Insects Food Feed 2023;9(4):399–414. https://doi.org/10.3920/JIFF2022.0055.
[41] Sheppard DC, Tomberlin JK, Joyce JA, Kiser BC, Sumner SM. Rearing methods for the black soldier fly (Diptera: Stratiomyidae). J Med Entomol 2002;39(4):695–8. https://doi.org/10.1603/0022-2585-39.4.695.
[42] Jiang P, Ergu D, Liu F, Cai Y, Ma B. A Review of Yolo algorithm developments. Procedia Comput Sci 2022;199:1066–73. https://doi.org/10.1016/j.procs.2022.01.135.
[43] Manduca G, Padovani L, Carosio E, Graziani G, Stefanini C, Romano D. Development of an Autonomous Fish-Inspired Robotic Platform forAquaculture Inspection and Management. In 2023 IEEE International Workshop on Metrology for Agriculture and Forestry (MetroAgriFor). IEEE; 2023, November. p. 188–93. https://doi.org/10.1109/MetroAgriFor58484.2023.10424093.
[44] Palanivel N, Deivanai S, Sindhuja B. The Art of YOLOv8 Algorithm in Cancer Diagnosis using Medical Imaging. In 2023 International Conference on System, Computation, Automation and Networking (ICSCAN). IEEE; 2023. p. 1–6. https://doi.org/10.1109/ICSCAN58655.2023.10395046.
[45] Farnebäck G. Two-frame motion estimation based on polynomial expansion. In: Image Analysis: 13th Scandinavian Conference (SCIA). Berlin Heidelberg: Springer; 2003. p. 363–70. https://doi.org/10.1007/3-540-45103-X_50.
[46] Kaur R, Singh S. A comprehensive review of object detection with deep learning. Digital Signal Process 2023;132:103812. https://doi.org/10.1016/j.dsp.2022.103812.
[47] Diaba SY, Elmusrati M. Proposed algorithm for smart grid DDoS detection based on deep learning. Neural Netw 2023;159:175–84. https://doi.org/10.1016/j.neunet.2022.12.011.
[48] Miller BS, Madhusudhana S, Aulich MG, Kelly N. Deep learning algorithm outperforms experienced human observer at detection of blue whale D-calls: a double-observer analysis. Remote Sens Ecol Conserv 2023;9(1):104–16. https://doi.org/10.1002/rse2.297.
[49] Santaera G, Zeni V, Manduca G, Canale A, Mele M, Benelli G, et al. Development of an autonomous smart trap for precision monitoring of hematophagous flies on cattle. Smart Agric Technol 2025;10:100842. https://doi.org/10.1016/j.atech.2025.100842.
[50] Arista-Jalife A, Nakano M, Garcia-Nonoal Z, Robles-Camarillo D, Perez-Meana H, Arista-Viveros HA. Aedes mosquito detection in its larval stage using deep neural networks. Knowl-Based Syst 2020;189:104841. https://doi.org/10.1016/j.knosys.2019.07.012.

[51] Picek L, Šulc M, Patel Y, Matas J. Plant recognition by AI: Deep neural nets, transformers, and kNN in deep embeddings. Front Plant Sci 2022;13:787527. https://doi.org/10.3389/fpls.2022.787527.
[52] Fu X, Ma Q, Yang F, Zhang C, Zhao X, Chang F, et al. Crop pest image recognition based on the improved ViT method. Information Processing in Agriculture 2024;11 (2):249–59. https://doi.org/10.1016/j.inpa.2023.02.007.
[53] Manduca G, Zeni V, Casadei A, Benelli G, Stefanini C, Romano D. Integrating Microfluidics and Deep Learning to Investigate Entomopathogenic Nematode Responses to Host Cues. In 2024 46th Annual International Conference of the IEEE Engineering in Medicine and Biology Society (EMBC). IEEE; 2024, July. p. 1–4. https://doi.org/10.1109/EMBC53108.2024.10782918.
[54] Tsolakis NK, Keramydas CA, Toka AK, Aidonis DA, Iakovou ET. Agrifood supply chain management: A comprehensive hierarchical decision-making framework and a critical taxonomy. Biosyst Eng 2014;120:47–64. https://doi.org/10.1016/j.biosystemseng.2013.10.014.
[55] Pratap V, Bombaywala S, Mandpe A, Khan SU. Solid waste treatment: Technological advancements and challenges. In: Soft Computing Techniques in Solid Waste and Wastewater Management. Elsevier; 2021. p. 215–31. https://doi.org/10.1016/B978-0-12-824463-0.00014-8.
[56] Ansari A, Pranesti A, Telaumbanua M, Ngadisih N, Hardiansyah MY, Alam T, et al. Optimizing water-energy-food nexus: achieving economic prosperity and environmental sustainability in agriculture. Front Sustainable Food Syst 2023;7: 1207197. https://doi.org/10.3389/fsufs.2023.1207197.
[57] Mitchell CA. Bioregenerative life-support systems. Am J Clin Nutr 1994;60(5): 820S–S824. https://doi.org/10.1093/ajcn/60.5.820S.
[58] Häder DP, Braun M, Hemmersbach R. Bioregenerative Life Support Systems in Space Research. In: Gravitational Biology I. SpringerBriefs in Space Life Sciences. Cham: Springer; 2018. https://doi.org/10.1007/978-3-319-93894-3_8.
[59] Liu H, Yao Z, Fu Y, Feng J. Review of research into bioregenerative life support system(s) which can support humans living in space. Life Sci Space Res 2021;31: 113–20. https://doi.org/10.1016/j.lssr.2021.09.003.
[60] Verbeelen T, Leys N, Ganigué R, Mastroleo F. Development of nitrogen recycling strategies for bioregenerative life support systems in space. Front Microbiol 2021; 12:700810. https://doi.org/10.3389/fmicb.2021.700810.

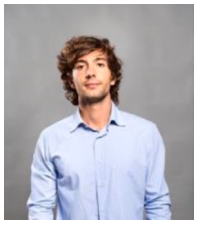

Gianluca Manduca [M.Sc. in Automation and Control Eng.] is a PhD student at The BioRobotics Institute of Scuola Superiore Sant'Anna of Pisa. Gianluca graduated in Automation and Control Engineering at Politecnico di Milano; before embarking on his PhD path, he spent a period as a visiting scholar at the Center for Automotive Research (CAR) of The Ohio State University, Columbus, OH, USA. The background in automation and control formed during studies initially contributed to the automotive sector, with work related to autonomous driving and lithium-ion battery modeling. Currently, Gianluca deals with biorobotic systems and biosensors managed through artificial intelligence techniques, with application to underwater robots and environmental monitoring. He is involved in several national and international research projects. gianluca.manduca@santannapisa.it.

Lloyd T. Wilson [B.Sc. in Entomology, PhD in Entomology] is Professor, Center Director and Jack B. Wendt Endowed Chair in Rice Research at the Texas A&M AgriLife Research and Extension Center at Beaumont. He published over 250 papers, the majority being peer-reviewed journal articles. He has been an Editor of a number of Journals. Earlier in my career, my research focused on assessing the abundance and spatial pattern of herbivores and their natural enemies, and quantifying crop-herbivore-natural enemy interactions. His current research largely focuses on 1) cultivar specific traits that affect diurnal and seasonal pattern of light interception, 2) interaction of phenotypic traits as they affect crop, growth, development, and yield, 3) crop model- and marker-assisted breeding, 4) pest host selection and dispersal, and 5) life cycle analysis of agricultural systems. lt-wilson@aesrg.tamu.edu.

CesareStefanini [M.Sc. in Mech. Eng. (honors), PhD in Microengineering (honors)] is Full Professor of Bioengineering at The BioRobotics Institute of Scuola Superiore Sant'Anna of Pisa, Italy, with the role of Institute Director and Area Leader in "Creative Engineering Design". His research activity is applied to different fields, including biomechatronics, and micromechatronics for medical and industrial applications. He received international recognitions for the development of novel actuators for microrobots and he has been visiting researcher at the University of Stanford, Center for Design Research, and Professor at Khalifa University, UAE. cesare.stefanini@santannapisa.it.

Donato Romano [M.Sc. in Agriculture, Food, and Environment Science and Technology (honors), PhD in BioRobotics (honors)] is currently Associate Professor at The BioRobotics Institute of Scuola Superiore Sant'Anna of Pisa, Italy, where he coordinates the Bio-Robotic Ecosystems Laboratory. Romano is mainly focusing his activities on bioinspired and biomimetic robotics, and in particular on animal-robot interaction, biohybrid systems, natural and biohybrid intelligence, ethorobotics, neuroethology. Romano received national and international recognitions for his research. He also has been visiting researcher at Khalifa University, Abu Dhabi (UAE). He is Member of the Editorial Board for many International Scientific Journals. Romano is Coordinator, PI, or partner of several national and international research projects. donato.romano@santannapisa.it.